# The boundary of the Milnor fiber of the singularity $f(x,y)+zg(x,y)=0$

Baldur Sigurðsson [1]

**Abstract**

Let $f, g \in \mathbb{C}\{x,y\}$ be germs of functions defining plane curve singularities without common components in $(\mathbb{C}^2, 0)$ and let $\Phi(x,y,z) = f(x,y) + zg(x,y)$. We give an explicit algorithm producing a plumbing graph for the boundary of the Milnor fiber of $\Phi$ in terms of a common resolution for $f$ and $g$. We give an example of a choice for $f$ and $g$ yielding a boundary of a Milnor fiber having more than one irreducible component.

## 1 Introduction

It is known that the boundary of the Milnor fiber of any hypersurface singularity in $(\mathbb{C}^3, 0)$ is a plumbed manifold. This was stated by Michel and Pichon in [6] and proved by separate methods by Némethi and Szilárd [12] and Michel and Pichon [7]. A stronger statement for certain real analytic map germs was proved by de Bobadilla and Neto [5]. As these theorems rely on resolution of singularities, they do not easily provide an explicit description of a plumbing graph describing the boundary. Calculations have been carried out, however for some particular singularities and families: for Hirzebruch singularities [8], suspensions of isolated plane curves [9] and in the many examples of [12].

In the case of a hypersurface singularity given by the equation

$$\Phi(x,y,z) = f(x,y) + zg(x,y) = 0,$$

where $f, g$ are singular germs with no common factors (but not necessarily reduced), we give an explicit algorithm producing a plumbing graph for the boundary of the Milnor fiber in terms of the graph associated with an embedded resolution of the plane curve singularities defined by $f$ and $g$. For the explicit statement, see theorem 6.3 and the construction in section 6. Furthermore, the algorithm provides a multiplicity system associated with the function $z$ described in section 7. This is obtained from an explicit description of the Milnor fiber by the author [14]. Singularities of the form $f(x,y) + zg(x,y)$ are closely related to the deformation theory of sandwitched singularities, see [3]. The article is organized as follows.

In section 2 we recall the results of [14] and fix notation related to the resolution graph of $f$ and $g$.

In section 3 we define plumbed manifolds and prove some useful lemmas related to them.

In section 4 we introduce families of multiplicities and dual multiplicities assigned to a complex valued function on a plumbed 3-manifold, satisfying certain conditions. In the case of a fibration over $S^1$, these multiplicities coincide with the multiplicities used in [4, 12].

[1] Universidad Nacional Autónoma de México, baldur@im.unam.mx. The author was partially supported by the ERCEA 615655 NMST Consolidator Grant, by the Basque Government through the BERC 2014-2017 program and by the Spanish Ministry of Economy and Competitiveness MINECO: BCAM Severo Ochoa excellence accreditation SEV-2013-0323 during the writing of this article.

In section 5 we prove a useful lemma relating the negative continued fraction expansion of a rational number to a plumbing construction.

In section 6 and section 7 we provide the details of the construction of the plumbing graph for the boundary of the Milnor fiber of $\Phi$ and the families of multiplicities and dual multiplicities for the coordinate function $z$. These statements can be read after only reading definition 2.1.

In section 8 we provide some examples. First we give the simple plumbing graph describing boundary of the Milnor fiber of a $T_{a,b,*}$ singularity given by the equation $x^a + y^b + xyz = 0$. This example is discussed in [12] 22.2.

Section 9 contains proofs of theorem 6.3 and theorem 7.1.

**1.1 Notation and conventions.** (i) We denote by $D \subset \mathbb{C}$ the open unit disk and by $\overline{D}$ the closed unit disk. We also set $S^1 = \partial\overline{D}$. For any $r > 0$, let $D_r, \overline{D}_r, S^1_r$ be the corresponding disks and circle with radius $r$.

(ii) If $X$ is a manifold, and $C \subset X$ is a submanifold of dimension $d$, then we denote by $[C] \in H_d(M, \mathbb{Z})$ the associated homology class. If $X$ is a compact oriented compact manifold, possibly with boundary, we denote by $(\cdot,\cdot)_X$ the intersection pairing between $H_i(X, \mathbb{Z})$ and $H_{n-i}(X, \partial X, \mathbb{Z})$, where $n = \dim X$. In particular, if $\partial X = \emptyset$ and $i = n/2$, then $(\cdot,\cdot)_X$ is the intersection form on the middle homology.

(iii) The boundary of an oriented manifold is oriented by the usual *outward-pointing-vector first* rule. Note that if a codimension one submanifold $N \subset M$ splits $M$ into two pieces, this rule induces opposite orientations according to which piece is chosen.

(iv) A locally trivial differential fiber bundle with a chosen orientation on the total space and the base space induces an orientation on each fiber by the following requirement. A lifting of a positive basis of the tangent space of the base space, followed by a positive basis of the tangent space of the fiber yields a positive orientation of the total space. In fact, this rule induces an orientation on the fibers, the total space or the base space, given orientations on the other two.

**Acknowledgements.** I would like to thank Némethi András for suggesting this problem to me and for the many helpful discussions we have had.

## 2 The Milnor fiber

In [14] the author gives a description of the Milnor fiber $F_\Phi$ of the singularity $\Phi(x, y, z) = f(x, y) + zg(x, y) = 0$. We will now recall that result and fix some notation.

**2.1 Definition.** Let $\phi : V \to \mathbb{C}^2$ be a common resolution of the functions $f$ and $g$ with exceptional divisor $E$, decomposing into irreducible components as $E = \cup_{v\in\mathcal{W}} E_v$ and denote by $\Gamma$ the associated embedded resolution graph. The set of vertices in $\Gamma$ is $\mathcal{V} = \mathcal{W} \amalg \mathcal{A}$, where $\mathcal{W}$ corresponds to components of the exceptional divisor, while elements of $\mathcal{A}$ are *arrowheads*, corresponding to components of the strict transforms of $f$ and $g$. For any $a \in \mathcal{A}$ there is a $w_a \in \mathcal{W}$ so that $\{w_a, a\}$ is an edge in $\Gamma$. Write $\mathcal{A} = \mathcal{A}_f \amalg \mathcal{A}_g$, where elements of $\mathcal{A}_f$ and $\mathcal{A}_g$ correspond to components of the strict transform of $f$ and $g$, respectively.

For $v \in \mathcal{V}$, we denote by $m_v$ and $l_v$ the multiplicities of $f$ and $g$, respectively. In particular, $m_v = 0$ if and only if $v \in \mathcal{A}_g$ and, similarly, $l_v = 0$ if and only if $v \in \mathcal{A}_f$.

Define $\mathcal{W}_1 = \{w \in \mathcal{W} \,|\, m_w \leq l_w\}$ and $\mathcal{W}_2 = \{w \in \mathcal{W} \,|\, m_w > l_w\}$. Write $\mathcal{A}_i = \{a \in \mathcal{A} \,|\, w_a \in \mathcal{W}_i\}$ for $i = 1, 2$. Similarly, take $\mathcal{A}_{f,i}, \mathcal{A}_{g,i} \subset \mathcal{A}_i$ so that $\mathcal{A}_f = \mathcal{A}_{f,1} \amalg \mathcal{A}_{f,2}$ and $\mathcal{A}_g = \mathcal{A}_{g,1} \amalg \mathcal{A}_{g,2}$.

**2.2 Definition.** For $w \in \mathcal{W}$, let $T_w$ be a tubular neighbourhood around $E_w$ in $V$ and let $T = \cup_{w \in \mathcal{W}} T_w$. Set also $T_i = \cup_{w \in \mathcal{W}_i} T_w$ for $i = 1, 2$. For a given $0 < \varepsilon \ll 1$, let $F_f = f^{-1}(\varepsilon)$ be the Milnor fiber of $f$, and $F'_f = \phi^{-1}(F_f)$ its pullback to $V$. Let $T_\varepsilon$ be a small tubular neighbourhood around $F'_f$ in $T$. We also choose tubular neighbourhoods $T_a \subset T$ around $E_a$ for any $a \in \mathcal{A}$. With these choices fixed, choose a small tubular neighbourhood $T' = \cup_{w \in \mathcal{W}} T'_w$ around the exceptional divisor inside $T$. This is chosen small enough that $T' \cap T_\varepsilon = \emptyset$.

Set $T_{f,i} = \cup_{a \in \mathcal{A}_{f,i}} T_a$, and $T_{g,i} = \cup_{a \in \mathcal{A}_{g,i}} T_a$ for $i = 1, 2$ and let

$$\overline{T}_{f,g} = (\overline{T}_{f,1} \setminus T') \cup \overline{T}_\varepsilon \cup (\overline{T}_2 \setminus (T' \cup T_{g,2})).$$

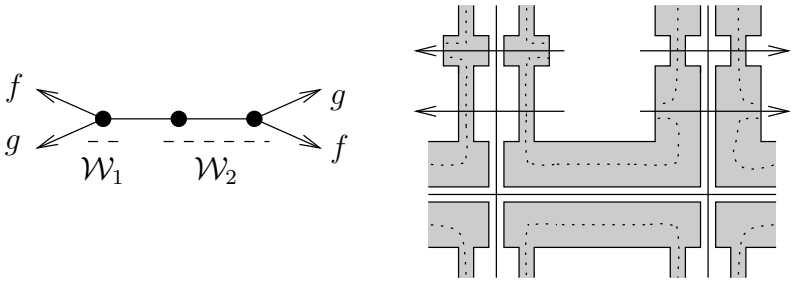


Figure 1: A schematic picture showing $\overline{T}_{f,g}$. The Milnor fiber of $f$ is shown as a dotted curve. The Milnor fiber of $\Phi$ is obtained by twisting along the strict transform of $g$.

**2.3 Definition.** Let $X$ be a four dimensional manifold with boundary and $\iota : \overline{D} \to X$ an embedding of the closed disk into $X$ such that $\iota$ sends $S^1 = \partial\overline{D}$ to $\partial X$ and the image of $\overline{D}$ is transversal to $\partial X$. Then there exists a map $\psi : \overline{D} \times \overline{D} \to X$ parametrizing a tubular neighbourhood of $\iota(D)$ in $X$ so that $\psi(0, z) = \iota(z)$ for $z \in \overline{D}$ and $\psi(x, z) \in \partial X$ for $x \in \overline{D}$ and $z \in S_1 = \partial D$. For $k \in \mathbb{Z}$, the $k^{\text{th}}$ *twist* along $\iota$ is defined as $(X \setminus \psi(D \times \overline{D})) \amalg_{t_k} \overline{D} \times \overline{D}$ where the glueing map $t_k : S^1 \times \overline{D} \to (X \setminus \psi(D \times \overline{D}))$ is defined by $t_k(x, z) = \psi(x, x^k z)$ and is denoted by $X_{\iota,k}$. We also say that $X_{\iota,k}$ is obtained from $X$ by *twisting* $X$ *k times along* $\iota(\overline{D})$.

**2.4 Definition.** In [14], the author shows that for any $a \in A_g$, the intersection $E_a \cap \overline{T}_{f,g}$ is a disjoint union of $m_{w_a}$ disks embedded in $\overline{T}_{f,g}$. Let $F_{f,g}$ be the manifold obtained from $\overline{T}_{f,g}$ by twisting each of these disks $l_a$ times for all $a$.

**2.5 Theorem** ([14])**.** *The Milnor fiber $F_\Phi$ is diffeomorphic to $F_{f,g}$.* ■

**2.6 Definition.** Let $M_{f,g} = \partial F_{f,g}$. We also set $M'_{f,g} = \partial\overline{T}_{f,g}$.

## 3 Plumbed 3-manifolds

In this section we give an introduction to plumbed three manifods and plumbing graphs, along with some useful properties. Throughout this text, an $S^1$-bundle will mean a principal $S^1$-bundle. In particular, we assume that there is a consistent choice for orientation on each fiber. In fact, all our $S^1$-bundles will have as base space an *oriented* real surface. This determines a consistent choice of orientation on fibers as described in 1.1(iii).

We note that apart from our restriction on orientability, our definition of a plumbed manifold is equivalent to the definition in [13]. This can be seen from lemma 3.8. We note, however, that our construction differs slightly to the standard one. This is explicated in remark 3.9. The main reason for this is that in our construction in section 9, we identify the three dimensional plumbed pieces directly, but the result can in no natural way be seen as the boundary of a four dimensional plumbed manifold (as is the case for links of isolated surface singularities).

**3.1 Definition.** A *plumbed manifold* is a three dimensional compact manifold $M$, possibly with boundary, given as a union of submanifolds with boundary $M = \cup_{v\in\mathcal{W}} M_v$ having the following properties.

(i) For each $v, w \in \mathcal{W}$, $v \neq w$ we have an $e_{v,w} \in \mathbb{N}$ so that

$$M_v \cap M_w = \amalg_{i=1}^{e_{v,w}} S_{v,w,i},$$

with $S_{v,w,i}$ an embedded torus $M \supset S_{v,w,i} \cong S^1 \times S^1$. Thus, $S_{v,w,i}$ is a component of $\partial M_v$ and inherits an orientation. Since $e_{v,w} = e_{w,v}$, we can assume that as sets, we have $S_{w,v,i} = S_{v,w,i}$ for $i = 1, \ldots, e_{v,w}$.

(ii) For each $v$ we have a compact connected surface $\Sigma_v$ (possibly with boundary) and a locally trivial $S^1$ bundle $\pi_v : M_v \to \Sigma_v$. If $1 \leq i \leq e_{v,w}$ for some $w \neq v$, then $S_{v,w,i} = \pi^{-1}(B_{v,w,i})$ where $B_{v,w,i} \cong S^1$ is a component of the boundary of $\Sigma_v$.

(iii) Assume that $1 \leq i \leq e_{v,w}$ for some $v \neq w$. The map

$$S_{v,w,i} \to B_{v,w,i} \times B_{w,v,i}, \quad p \mapsto (\pi_v(p), \pi_w(p))$$

is a diffeomorphism.

(iv) For each $v \in \mathcal{V}$, let $B_{v,1}, \ldots, B_{v,e_v}$ be the components of $\partial\Sigma_v$ not of the form $B_{v,w,i}$ for some $w, i$. We assume that a section $s_{v,i} : B_{v,i} \to \Sigma_v$ to the reduced bundle $\pi_v|_{B_{v,i}}$ is given.

**3.2 Remark.** The sections $s_{v,i}$ are not part of the plumbing structure defined in [13]. This means that if $M_v$ contains a component of the boundary of $M$, then $v$ has no well defined Euler number. In our algorithm, the final output is a manifold without boundary, but in order to construct it we will have to glue together manifolds along boundaries. This is done most easily by keeping track of sections trivializing the fibration $M_v \to \Sigma_v$ over boundary components.

**3.3.** We orient $S_{v,w,i}$ by considering it as a subset of the boundary of $M_v$. This way, $S_{v,w,i} = S_{w,v,i}$ as sets, but $S_{v,w,i} = -S_{w,v,i}$ as oriented manifolds. We also orient the boundary of $\Sigma_w$ by the same rule, for any $w \in \mathcal{W}$.

**3.4.** For a closed surface $\Sigma$, the *Euler number* classifies the $S^1$ bundles over $\Sigma$. However, every $S^1$ bundle $\pi : M \to \Sigma$ over a compact surface with nonempty boundary is trivial. But given a trivialization, or, equivalently, a section $s : \partial\Sigma \to \partial M$, over the boundary, a *relative Euler number* is well defined, and invariant under homotopy of the section. This is a complete invariant in the following sense. Let $\Sigma$ be a compact surface with boundary and take two $S^1$ bundles $M, M' \to \Sigma$ with sections $s : \partial\Sigma \to \partial M$ and $s' : \partial\Sigma \to \partial M'$ and an isomorphism of bundles $\psi : M|_{\partial\Sigma} \to M'|_{\partial\Sigma}$ sending $s$ to $s'$. Then $\psi$ extends to an isomorphism of bundles $M \to M'$ if and only if the relative Euler numbers coincide. We will refer to the relative Euler number simply as the Euler number.

The relative Euler number is defined as follows. Let $D \subset \Sigma$ be an open disk. We can extend the section $s : \partial\Sigma \to \partial M$ to a section $\overline{s} : \Sigma \setminus D \to M \setminus \pi^{-1}(D)$. Given an orientation preserving diffeomorphism $\varphi : \partial D \to S^1$, there is a unique number $b \in \mathbb{Z}$ so that the twisted section $\overline{s}^b : \partial D \to \pi^{-1}(\partial D)$, $x \mapsto \varphi(x)^b \overline{s}(x)$ extends over the disk $D$. The relative Euler number is defined as $-b$.

**3.5 Lemma.** *Let $M \to \Sigma$ be an $S^1$ bundle over a compact surface with boundary. Let $-b$ be its the Euler number relative to a section $s : \partial\Sigma \to M$. Let $C \subset M$ be a fiber of the bundle and $C'$ the image of $s$ (as* oriented *submanifolds). Then, in $H_1(M, \mathbb{Z})$*

$$-b[C] = [C']. \tag{3.1}$$

*Proof.* This follows from the definition of the relative Euler number. Indeed, let $\overline{s} : \Sigma \setminus D \to M$ be a section as above. It follows that $[C'] - \overline{s}_*[\partial D] = 0$. The sign comes from the fact that $\partial D$ is oriented as the boundary of the disk $D$, which is the opposite to the orientation inherited from the complement of the disk. Since the section $\overline{s}^b_*$ extends over $D$ and $D$ is null-homotopic, the map $\overline{s}^b : \partial D \to M$ is homotopic to a constant map $\partial D \to M$. It follows that $\overline{s}_*[\partial D] = -b[C]$. ■

**3.6 Remark.** If $\partial\Sigma \neq \emptyset$, then eq. 3.1 can be taken as an alternative definition of the (relative) Euler number. Indeed, it follows from the Künneth formula that the $[C]$ is not a torsion element of $H_1(M, \mathbb{Z})$.

**3.7 Definition.** A *plumbing graph* is a decorated graph $G$ (with no loops) with vertex set $\mathcal{V} = \mathcal{W} \amalg \mathcal{A}$, where each vertex $a \in \mathcal{A}$ has a unique neighbour $w_a$ and $w_a \in \mathcal{W}$. We refer to vertices in $\mathcal{A}$ as *arrowhead vertices*. $G$ is decorated as follows.

- ❀ For each $w \in \mathcal{W}$, we have integers $-b_w \in \mathbb{Z}$ and $g_v \in \mathbb{Z}_{\geq 0}$. These are referred to as the associated *Euler number* (or sometimes *selfintersection number*) and the *genus*.
- ❀ Each edge $e$ connecting two vertices in $\mathcal{W}$ is given a sign $\varepsilon_e \in \{+, -\}$.

In a drawing of a graph, the genus $g_v$ is written within square brackets as $[g_v]$ to be distinguished from the Euler number. If it is omitted, it is assumed to be 0. A negative edge will be indicated by the symbol $\ominus$, whereas if indication is omitted, the sign is assumed to be positive. An edge connecting $w \in \mathcal{W}$ and an arrowhead $a \in \mathcal{A}$ is drawn as a dashed edge, see e.g. fig. 2.

Let $M = \cup_{v \in \mathcal{W}} M_i$ be a plumbed manifold and use the notation introduced in definition 3.1. The *associated plumbing graph* $G$ has vertex set $\mathcal{V} = \mathcal{W} \amalg \mathcal{A}$ where $\mathcal{A} = \amalg_{v \in \mathcal{W}} \mathcal{A}_v$, where the elements of $\mathcal{A}_v$ correspond to the boundary

components $B_{v,1}, \ldots, B_{v,e_v}$ of $\Sigma_v$. It has $e_{v,w}$ edges connecting $v$ and $w$ if $v, w$ are distinct elements of $\mathcal{W}$ and a single edge connecting any $a \in \mathcal{A}_w$ with $w$ if $w \in \mathcal{W}$, and no other edges. Denote by $\mathcal{E}$ this set of edges. For a $v \in \mathcal{W}$, there is an obvious correspondence between edges adjacent to $v$ and boundary components of $M_v$, and these embed in $M$. For each $e \in \mathcal{E}$, let $S_e$ be the corresponding torus embedded in $M$.

The genus $g_v$ is the genus of the surface $\Sigma_v$. The Euler number $-b_v$ is the Euler number of the $S^1$ bundle $M_v \to \Sigma_v$, trivialized on the boundary components $B_{v,i}$ by the given section, and on the components $B_{v,w,i}$ by any fiber of $S_{v,w,i} = S_{w,v,i} \to B_{w,v,i}$.

Any edge $e \in \mathcal{E}$ connecting $v, w \in \mathcal{W}$ corresponds to a component $S_{v,w,i} = S_{w,v,i}$ of the intersection $M_v \cap M_w$. Take fibers $C_v$ and $C_w$ of $\pi_v$ and $\pi_w$, respectively, contained in $S_{v,w,i}$. The sign $\varepsilon_e$ is defined as the intersection number of $C_v$ and $C_w$ in $S_{v,w,i}$, that is,

$$\varepsilon_e = ([C_v], [C_w])_{S_{v,w,i}}.$$

It follows from definition that this intersection number is $\pm 1$. This sign depends on the orientation on $S_{v,w,i}$, which, we recall, is obtained by viewing $S_{v,w,i}$ as a subset of $\partial M_v$.

**3.8 Lemma.** *Let $v, w$ be vertices connected by an edge $e$ in a plumbing graph associated to a plumbed manifold $M$. Let $C_w$ be a fiber of $\pi_w$ contained in the torus $S_{v,w,i}$ corresponding to $e$. Then the sign $\varepsilon_e$ is positive if and only if $-C_w$ is an oriented section to the map $S_{v,w,i} \to B_{v,w,i}$.*

*Proof.* Let $C_v \subset S_{v,w,i}$ be a fiber of $\pi_v$. We have $\varepsilon_e = ([C_v], [C_w])_{S_{v,w,i}}$. Therefore, if $B$ is the oriented image of some section of $\pi_v|_{S_{v,w,i}}$, then it suffices to show that $([C_v], [B])_{S_{v,w,i}} = -1$. By construction, $C_v$ and $B$ intersect in a single point, say $x \in S_{v,w,i}$, and we can assume that this intersection is transverse. Let $c, b \in T_x S_{v,w,i}$ be tangent vectors inducing positive bases of $T_x C_v$ and $T_x B_v$. Let $a \in T_x M_v$ be an outward pointing tangent vector. By definition, $(\pi_v(a), \pi_v(b))$ is a positive basis of $T_{\pi_v(x)} B_{v,w,i}$. Therefore, $(a, b, c)$ is a positive basis of $T_x M_v$, and so $(b, c)$ is a positive basis of $T_x S_{v,w,i}$. This means that $([B], [C_v])_{S_{v,w,i}} = 1$ and so $([C_v], [B])_{S_{v,w,i}} = -1$. ∎

**3.9 Remark.** The above lemma may seem contrary to the usual definition of plumbing [13, 12]. There, the authors start with $S^1$-bundles over a closed surfaces. The glueing of two pieces, corresponding to an edge $e$, is made by removing a tubular neighbourhood around a fiber in each piece and identifying the boundaries by switching meridians and fibers, multiplied with a sign $\varepsilon_e$. The output of the two constructions is identical, but the submanifold $B$ in the proof above, is a meridian, but with the opposite orientation to that of a standard meridian.

**3.10 Example.** [10, 12] Let $\tilde{X}$ be a smooth complex surface and let $E \subset \tilde{X}$ be a compact *normal crossing divisor*. This means that $E$ is a compact reduced analytic subspace of pure dimension one, decomposing as $E = \cup_{v \in \mathcal{V}} E_v$ into irreducible components, with the condition that each $E_v$ is a submanifold of $\tilde{X}$, that each $E_v$ and $E_w$ intersect transversally, and that any singularity of $E$ is a double point. If $T \subset \tilde{X}$ is a suitable small neighbourhood of $E$, then $M = \partial T$ is a plumbed manifold, whose plumbing graph $G$ is given by the intersection

matrix of $E$, that is, $G$ has vertex set $\mathcal{V}$, the genus $g_v$ is the genus of $E_v$, the Euler number $-b_v$ is the selfintersection number $(E_v, E_v)$, equivalently, it is the Euler number of the normal bundle of the embedding $E_v \hookrightarrow \tilde{X}$, and the number of edges between $v, w \in \mathcal{V}$ is the cardinality $|E_v \cap E_w|$. Furthermore, $\varepsilon_e = +$ for any edge $e$.

**3.11.** A plumbed manifold $M$ can be recovered from its (decorated) plumbing graph $G$ as follows. As before, denote by $\mathcal{V}$ and $\mathcal{E}$ the set of vertices and edges in $G$, and by $g_v$ and $-b_v$ the genus and the selfintersecion number of a vertex $v$ and by $\varepsilon_e$ the sign of an edge. For each $v \in \mathcal{V}$, let $\Sigma_v$ be a compact surface of genus $g_v$ with $e_v + \sum_{w \in \mathcal{V} \setminus \{v\}} e_{v,w}$ boundary components, give names $B_{v,w,i}$, for $w \in \mathcal{V} \setminus \{v\}$ and $1 \leq e_{v,w}$ and $B_{v,i}$ for $1 \leq i \leq e_v$. Let $\pi_v : M_v \to \Sigma_v$ be an $S^1$ bundle with sections $s_{v,w,i}$ and $s_{v,i}$ over the boundary inducing Euler number $-b_v$. The section $s_{v,w,i}$ induces a trivialization $\phi_{v,w,i} : S^1 \times S^1 \to \pi_v^{-1}(B_{v,w,i})$.

We then have $M \cong \amalg_{v \in \mathcal{V}} M_v / \sim$ where $\sim$ is the equivalence relation on $\amalg_{v \in \mathcal{V}} M_v$ generated by $\phi_{v,w,i}(\theta_1, \theta_2) \sim \phi_{w,v,i}(\theta_2^{-\varepsilon_e}, \theta_1^{-\varepsilon_e})$ where $e$ is the $i^{\text{th}}$ edge connecting $v$ and $w$. The negative sign in the exponents in the glueing map is explained by remark 3.9.

## 4 Multiplicities associated with complex valued functions

In this section we give a definition of multiplicities of a complex valued function on a plumbed manifold under some restrictions (see 4.1). This definition coincides with the multiplicities associated with fibred links in section 18 of [4], if the function is a fibration over $S^1$. These multiplicities are useful as they can be obtained by local computation, but can be used to determine Euler numbers, see lemma 4.3.

**4.1.** Let $M = \cup_{v \in \mathcal{V}} M_v$ be a plumbed manifold with graph $G$, with vertex set $\mathcal{V} = \mathcal{W} \cup \mathcal{A}$ and let $\zeta : M \to \mathbb{C}$ be a differentiable function having 0 as a regular value. Furthermore, assume that $\zeta$ does not vanish on $\partial M_v$ for all $v \in \mathcal{W}$. Thus, $N_v = \zeta^{-1}(0) \cap M_v$ is a closed submanifold of $M_v$ which does not intersect its boundary. Assume also that $N_v$ is homologous to a multiple of $[C_v]$ in $M_v$, that is, $[N_v] = n_v[\pi_v^{-1}(p)]$ for some (well defined) $n_v \in \mathbb{Z}$.

For any $x \in \Sigma_v \setminus \pi_v(N_v)$, there is a unique $m_x \in \mathbb{Z}$ so that $\zeta_*([\pi^{-1}(x)]) = m_x[S^1] \in H_1(\mathbb{C}^*)$. This number is a locally constant function of $x$. In fact, let $\xi : [0,1] \to \sigma$ be a 1-chain connecting $x = \xi(0)$ and $y = \xi(1)$. We can assume that $\xi$ is an embedding, and by a small perturbation, we can assume that the map $N_v \to \Sigma$, induced by $\pi_v$, is an immersion, transverse to $\xi$. At any intersection point of $\xi$ and $\pi_v(N_v)$, one sees that $m_{\xi(\cdot)}$ changes by $\pm 1$, depending on the sign of the intersection. In particular, if $x, y \in \partial\Sigma_v$, then $\xi$ is a cycle inducing an element $[\xi] \in H_1(\Sigma_v, \partial\Sigma_1, \mathbb{Z})$. It follows from the assumptions that we made that $\pi_{v,*}([N_v]) = 0 \in H_1(\Sigma, \mathbb{Z})$, and so

$$(\pi_{v,*}([N_v]), [\xi])_{\Sigma_v} = 0.$$

It follows that for $x, y \in \partial\Sigma$, the number $m_x = m_y$ is a number which is well defined by the map $\zeta$; we denote it by $m_v$.

**4.2 Definition.** Let $\zeta : M \to \mathbb{C}$ be as in 4.1. We refer to the families $(m_v)_{v \in \mathcal{V}}$ and $(n_w)_{w \in \mathcal{W}}$ (defined above) as the *family of multiplicities* and *dual family*

*of multiplicities* associated with $\zeta$, respectively. In a drawing of a plumbing graph, a multiplicity is written within parenthesis, whereas a dual multiplicity is written in parenthesis next to an arrow emanating from the vertex.

**4.3 Lemma.** *Let $\zeta : M \to \mathbb{C}$ be as in 4.1, and let $(m_v)_{v\in\mathcal{V}}$ and $(n_v)_{v\in\mathcal{W}}$ be the associated families of multiplicities and dual multiplicities. Let $w \in \mathcal{W}$. If $e \in \mathcal{E}_w$ connects $w$ and $v$, set $m_e = m_v$. We then have*

$$-b_w m_w + \sum_{e\in\mathcal{E}_w} \varepsilon_e m_e = n_v.$$

*Proof.* Let $C_w$ be a fiber of $\pi_w$. Since $M_w \cong \Sigma_w \times S^1$, the element $[C_w] \in H_1(M_w, \mathbb{Z})$ is nontorsion. It therefore suffices to show that

$$\left(-n_w - b_w m_w + \sum_{e\in\mathcal{E}_w} \varepsilon_e m_e\right)[C_w] = 0.$$

We can assume that $\zeta$ is transversal to the submanifold with boundary $\mathbb{R}_{\geq 0} \subset \mathbb{C}$ so that $\zeta|_{M_w}^{-1}(\mathbb{R}_{\geq 0})$ is a submanifold with boundary $K_w$ in $M_w$. Furthermore, we can assume that $K_w$ is transversal to $\partial M_w$. This way, $[\partial K_w] = -[N_w] + \sum_{e\in\mathcal{E}_w}[K_w \cap S_e] \in H_1(M_w, \mathbb{Z})$. Let $e \in \mathcal{E}_w$, connecting $w$ and $v \in \mathcal{V}$. Assume that the fiber $C_w$ was chosen so that $C_w \subset S_e$. Furthermore, let $C_v$ be a fiber of $\pi_v$ contained in $S_e$ if $v \in \mathcal{W}$, otherwise, let $C_v$ be the image of $s_v$. It follows from definition that

$$([K_e \cap S_e], [C_w])_{S_e} = m_w, \quad ([K_e \cap S_e], [C_v])_{S_e} = m_v.$$

Since $[C_v]$ and $[C_w]$ form a basis of $H_1(S_e, \mathbb{Z})$, and we have

$$([C_w], [C_w])_{S_e} = ([C_v], [C_v])_{S_e} = 0, \quad ([C_w], [C_v])_{S_e} = \varepsilon_e,$$

we get $[K_e \cap S_e] = \varepsilon_e(m_v[C_w] - m_w[C_v])$. This yields

$$\begin{aligned} 0 = [\partial K_e] &= -n_w[C_w] + \sum_{e\in\mathcal{E}_w} \varepsilon_e(m_v[C_w] - m_w[C_v]) \\ &= \left(-n_w - b_w m_w + \sum_{e\in\mathcal{E}_w} \varepsilon_e m_v\right)[C_w]. \end{aligned}$$

Here, the variable $v$ inside the sum depends on $e$. The last equality follows from lemma 3.5 ∎

**4.4 Example.** Let $\tilde{X}$ and $E = \cup_{v\in\mathcal{V}} E_v$ be as in example 3.10, and let $h : \tilde{X} \to \mathbb{C}$ be a holomorphic function. Decompose the divisor of $h$ as $(h) = (h)_{\text{exc}} + (h)_{\text{str}}$ so that $(h)_{\text{exc}}$ is supported on $E$, and $(h)_{\text{str}}$ has no components with nonzero coefficient included in $E$. We can then write $(h)_{\text{exc}} = \sum_{v\in\mathcal{V}} m_v E_v$, and $(h)_{\text{str}} = \sum_D n_D D$ with $n_D = 0$ if $D = E_v$ for some $v \in \mathcal{V}$. Assume that the support of $(h)_{\text{str}}$ does not contain any intersection points in $E$, that is, if $n_D \neq 0$, then $D \cap E_v \cap E_w = \emptyset$ for $v, w \in \mathcal{W}$, $v \neq w$. If $T \subset \tilde{X}$ is a small tubular neighbourhood around $E$, then $M = \partial T$ is a plumbed manifold and $h|_M$ satisfies the conditions in 4.1. The associated family of multiplicities is $(m_v)_{v\in\mathcal{W}}$. Furthermore, the family $(n_v)_{v\in\mathcal{V}}$ of dual multiplicities is given as the intersection $n_v = (E_v, (h)_{\text{str}})$.

Note that here we do not assume $(h)_{\text{str}}$ to be smooth, only that its intersection points with $E$ lie in the regular part of $E$.

## 5 Negative continued fractions

In this section we discuss negative continued fractions and a plumbing construction related to them. Some of the notation introduced in this section follows [2, III.5].

**5.1.** Let $a, b$ be relatively prime integers, $b > 0$. The fraction $a/b$ can be written in a unieque way as a (negative) continued fraction

$$\frac{a}{b} = k_1 - \frac{1}{k_2 - \frac{1}{\cdots - \frac{1}{k_s}}} \tag{5.1}$$

where $k_i \geq 2$ for $i \geq 2$. Further, we have $k_1 \geq 2$ if and only if $a > b$ and $k_1 > 0$ if and only if $a > 0$.

**5.2 Definition.** The rational number $a/b$ is called the *(negative) continued fraction* associated with the sequence $k_1, \ldots, k_s$ and is denoted by $[k_1, \ldots, k_s]$. The sequence $k_1, \ldots, k_s$ is called the *(negative) continued fraction expansion* of the rational number $a/b$.

**5.3.** Given $a/b = [k_1, \ldots, k_s]$ as above, define integers $\mu_i$ and $\tilde{\mu}_i$ for $0 \leq i \leq s+1$ as follows. Start by setting

$$\mu_0 = 0, \quad \mu_1 = 1, \quad \tilde{\mu}_0 = -1, \quad \tilde{\mu}_1 = 0.$$

Then, assuming that we have defined $\mu_j, \tilde{\mu}_j$ for $0 \geq j \geq i$ for some $i > 0$, define

$$\mu_{i+1} = k_i \mu_i - \mu_{i-1}, \quad \tilde{\mu}_{i+1} = k_i \tilde{\mu}_i - \tilde{\mu}_{i-1}.$$

Using induction, one finds

$$\begin{vmatrix} \mu_i & \mu_{i+1} \\ \tilde{\mu}_i & \tilde{\mu}_{i+1} \end{vmatrix} = 1, \quad i = 0, \ldots, s. \tag{5.2}$$

Furthermore, the numbers $\mu_i$ and $\tilde{\mu}_i$ are positive for $i > 1$ if $a > 0$. A simple induction on $s$ also proves $\mu_{s+1} = a$ and $\tilde{\mu}_{s+1} = b$.

**5.4 Lemma.** *Let $a, b$ be positive integers with no common factors, and let $k_i, \mu_i, \tilde{\mu}_i$ be defined as above. The manifold $M = \bar{D} \times S^1$ is a plumbed manifold, given as $M = \cup_{i=1}^{s} M_i$ where*

$$M_1 = D_{\frac{1}{s}} \times S^1, \quad M_i = (\bar{D}_{\frac{i+1}{s}} \setminus D_{\frac{i}{s}}) \times S^1, \, i = 2, \ldots, s.$$

*We set $\Sigma_1 = D_{\frac{1}{s}}$ and $\pi_1 : M_1 \to \Sigma_1$, $(rt_1, t_2) \mapsto rt_1$ where $r \in \mathbb{R}_{\geq 0}$ and $t_i \in S^1$, as well as $\Sigma_i = \bar{D}_{\frac{i}{s}} \setminus D_{\frac{i-1}{s}}$ for $i > 1$ and $\pi_i : M_i \to \Sigma_i$, $(rt_1, t_2) \mapsto r t_1^{\mu_i} t_2^{\tilde{\mu}_i}$ for $i > 1$. The section over $S^1 \subset \Sigma_s$ is given by $t \mapsto (t^{\tilde{\mu}_{s+1}}, t^{-\mu_{s+1}})$. The associated plumbing graph is shown in fig. 2.*

*Proof.* It is clear that the given components intersect in tori. Furthermore, eq. 5.2 gives $\gcd(\tilde{\mu}_i, \mu_i) = 1$. It follows that $\pi_i$ is an $S^1$ fibration for all $i$. Another consequence of eq. 5.2 is that for $1 \leq i < s$, the map $\pi_i \times \pi_{i+1} : M_i \cap M_{i+1} \to S^1 \times S^1$ is a diffeomorphism and that fibers of $\pi_i$ and $\pi_{i+1}$

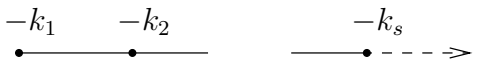


Figure 2: Plumbing representation of $S^1 \times \overline{D}$.

intersect positively in the torus $M_i \cap M_{i+1}$. The same equation shows that the map $t \mapsto (t^{\tilde{\mu}_{s+1}}, t^{-\mu_{s+1}})$ is really a section:

$$\pi_s(t^{\tilde{\mu}_{s+1}}, t^{-\mu_{s+1}}) = t^{\mu_s \tilde{\mu}_{s+1} - \tilde{\mu}_s \mu_{s+1}} = t.$$

Therefore, $M$ is a plumbed manifold with $s$ components. What is left to show is that the Euler number for the $i^{\text{th}}$ vertex, call it $v_i$, in the graph is $-k_i$. To see this, consider the function $\zeta : M \to \mathbb{C}$, $(z,t) \mapsto t$. The function does not vanish on $M$, and so the dual set of multiplicities vanish. We have parametrizations $S^1 \to M_i$, $t \mapsto (rt^{-\tilde{\mu}_i}, t^{\mu_i})$ of a fiber of $\pi_i$ for a suitable $r$. Thus, the multiplicities of $\zeta$ are given by $m_{v_i} = \mu_i$, and similarly, $m_a = \mu_{s+1}$, where $a$ is the arrowhead. Thus, by lemma 4.3, we have $-b_{v_i}\mu_i + \mu_{i-1} + \mu_{i+1} = 0$ for $1 \leq i \leq s$. Since the same equation holds with $b_{v_i}$ replaced with $k_i$ (and $\mu_i \neq 0$), we get $-b_{v_i} = -k_i$. ∎

## 6 Construction

In this section we state our main result in details. We construct a plumbing graph $G$ from the resolution graph $\Gamma$ along with the multiplicities $m_v$ and $l_v$ of $f$ and $g$. Theorem 6.3 says that this construction describes the boundary of the Milnor fiber of the hypersurface singularity given by $\Phi(x,y,z) = f(x,y) + zg(x,y)$.

Each of the first five steps of the algorithm is illustrated with the corresponding step in example 8.2. The full output of this example can be seen in fig. 14.

**6.1 Definition.** (i) Let $\Gamma'$ be a connected component of $\Gamma_1$, the induced subgraph of $\Gamma$ with vertex-set $\mathcal{W}_1$. Let $\mathcal{V}(\Gamma')$ be the vertex set of $\Gamma'$ and, for $v \in \mathcal{V}(\Gamma')$, let $\hat{\mathcal{E}}_v(\Gamma')$ be the set of edges connecting $v$ and a vertex in $\mathcal{A}_{f,1} \cup \mathcal{W}_2$. Set also $\hat{\mathcal{E}}(\Gamma') = \cup_{v \in \mathcal{V}(\Gamma')} \hat{\mathcal{E}}_v(\Gamma')$, and define $\hat{\mathcal{V}}(\Gamma')$ as the set of vertices in $\mathcal{A}_{f,1} \cup \mathcal{W}_2$ adjacent to edges in $\hat{\mathcal{E}}(\Gamma')$. For any edge $e \in \hat{\mathcal{E}}(\Gamma')$ connecting $v \in \mathcal{V}(\Gamma')$ and $w \in \mathcal{A}_{f,1} \cup \mathcal{W}_2$, set $v_e = v$ and $w_e = w$ and $m_e = \gcd(m_v, m_w)$. For $v \in \mathcal{V}(\Gamma')$, let $\hat{\delta}_v$ be the number of edges connecting $v$ and some vertex in $\mathcal{V}(\Gamma')$ or $\hat{\mathcal{V}}(\Gamma')$. Let $d_{\Gamma'} = \gcd_{v \in \mathcal{V}(\Gamma') \cup \hat{\mathcal{V}}(\Gamma')} m_v$ and define $g_{\Gamma'}, -b_{\Gamma'}$ by the equations

$$d_{\Gamma'}(2 - 2g_{\Gamma'}) = \sum_{v \in \mathcal{V}(\Gamma')} m_v(2 - \hat{\delta}_v) + \sum_{e \in \hat{\mathcal{E}}(\Gamma')} m_e, \tag{6.1}$$

$$d_{\Gamma'}(-b_{\Gamma'}) = \sum_{e \in \hat{\mathcal{E}}(\Gamma')} m_{v_e} l_{w_e} - m_{w_e} l_{v_e}. \tag{6.2}$$

Since $d_{\Gamma'} \neq 0$, these are well defined. As we will see later, we have $g_{\Gamma'}, -b_{\Gamma'} \in \mathbb{Z}$. The graph $G_{\Gamma'}$ has vertex set $\mathcal{W}(G_{\Gamma'}) = \{v_{\Gamma',1}, \ldots, v_{\Gamma',d_{\Gamma'}}\}$, with each vertex decorated by the selfintersection number $-b_{\Gamma'}$ and genus $[g_{\Gamma'}]$. No two of these

vertices are connected by an edge. Define $G_1$ as the disjoint union of the graphs obtained in this way.

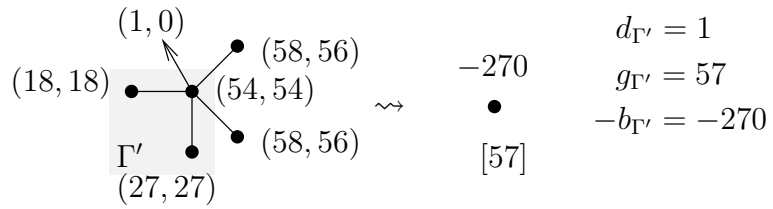


Figure 3: A connected component $\Gamma'$ of $\Gamma_1$ produces one vertex. The edges in $\hat{\mathcal{E}}(\Gamma')$ and vertices of $\hat{\mathcal{V}}(\Gamma')$ are also displayed.

(ii) Let $a \in \mathcal{A}_{f,1}$ and write $m_a/m_w = [k_1, \ldots, k_s]$. The graph $G_a$ has $2s+1$ vertices $v_{a,1,+}, \ldots, v_{a,s,+}, v_{a,1,-}, \ldots, v_{a,s,-}, v_{a,0}$. There is an edge with sign $\pm$ connecting $v_{a,i,\pm}$ and $v_{a,i+1,\pm}$ for each $1 \leq i \leq s-1$, as well as positive edges connecting $v_{a,0}$ and $v_{a,s,\pm}$. All these vertices have genus zero. The vertex $v_{a,i,\pm}$ has selfintersection $-b_{a,i,\pm} = \mp k_i$ and $v_{a,0}$ has selfintersection number $-b_{a,0} = 0$.

Define $G_{f,1}$ as the disjoint union of these graphs.

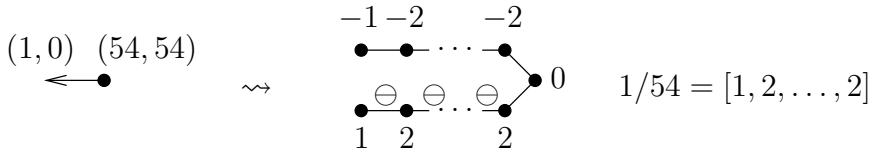


Figure 4: An arrowhead $a \in \mathcal{A}_{f,1}$ produces a subgraph of the final output. Note that in this case, since $m_a = 1$, all vertices other than the one to the right blow down. In any case, the minus signs on the lower bamboo can be removed by plumbing calculus.

(iii) Let $v_1 \in \mathcal{W}_1$ and $v_2 \in \mathcal{W}_2$ be vertices of $\Gamma$ connected by an edge $e$ and write $m_{v_2}/m_{v_1} = [k_1, \ldots, k_s]$. The graph $G_e$ has vertices $v_{e,1,+}, \ldots, v_{e,s,+}$, $v_{e,1,-}, \ldots, v_{e,s,-}, v_{e,0}$, each with genus zero. The vertex $v_{e,i,\pm}$ has the selfintersection number $-b_{e,i,\pm} = \mp k_i$ and $v_{e,0}$ has selfintersection $b_{e,0} = 0$. We have an edge with sign $\pm$ connecting $v_{e,i,\pm}$ and $v_{e,i+1,\pm}$, as well as positive edges connecting $v_{e,s,\pm}$ and $v_{e,0}$.

Let $G_{\mathrm{b}}$ be the disjoint union of graphs obtained in this way.

(iv) The graph $G_2$ is defined as follows. For each $w \in \mathcal{W}_2$, we have two vertices $v_{w,+}, v_{w,-}$ in $G_2$ and these are all the nonarrowhead vertices of $G_2$. They are decorated by genus zero and have selfintersection number $-b_{w,\pm} = \mp b_w$, where $-b_w$ is the selfintersection number of $w$ in $\Gamma$. For any edge $e$ connecting vertices $w, w' \in \mathcal{W}_2$, the vertices $v_{w,\pm}$ and $v_{w',\pm}$ are connected by an edge with sign $\pm$.

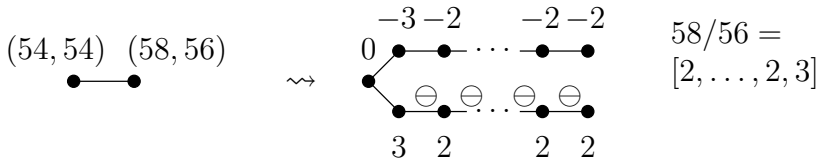


Figure 5: An edge connecting vertices from $\mathcal{W}_1$ and $\mathcal{W}_2$ induces a subgraph of the total output of the algorithm. In example 8.2, there are two such edges.

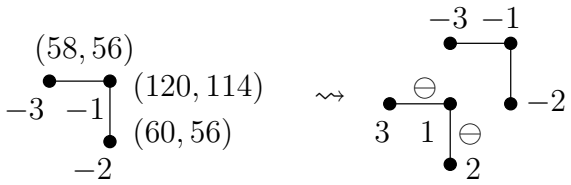


Figure 6: The above construction appears twice in example 8.2.

(v) Let $a \in \mathcal{A}_{g,2}$. The graph $G_a$ has nonarrowhead vertices $v_{a,0}, \ldots, v_{a,m_w}$ where $w = w_a$, each of genus zero. The vertex $v_{a,0}$ has selfintersection number $-b_{a,0} = 0$, whereas $v_{a,i}$ has selfintersection $-b_{a,i} = -l_a$. For each $1 \le i \le m_w$ there is a negative edge connecting $v_{a,0}$ and $v_{a,i}$.

Let $G_{g,2}$ be the disjoint union of graphs obtained in this way.

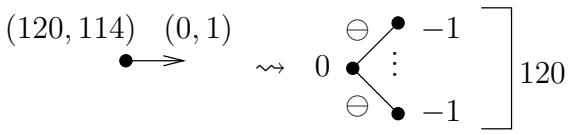


Figure 7: Part of the algorithm corresponding to an arrowhead $a \in \mathcal{A}_{g,2}$. Here, since $l_a = 1$, we can blow down the 120 vertices to the right, ending up with a single vertex with Euler number 120.

**6.2 Definition.** The graph $G$ is the disjoint union of the graphs $G_1$, $G_{f,1}$, $G_{\mathrm{b}}$, $G_2$, $G_{g,2}$, with the following additional edges.

(i) For $\Gamma' \subset \Gamma_1$ a connected component, $1 \le i \le d_{\Gamma'}$ and $a \in \mathcal{A}_{f,1}$, connect $v_{\Gamma',i}$ and $v_{a,0}$ with $m_e/d_{\Gamma'}$ negative edges, where $m_e$ is as in definition 6.1(i).

(ii) Similarly, assuming that $\Gamma' \subset \Gamma_1$ is a connected component, $1 \le i \le d_{\Gamma'}$ and that $v_1 \in \mathcal{W}(\Gamma')$ and $v_2 \in \mathcal{W}_2$ are connected by an edge $e \in \mathcal{E}(\Gamma)$. Connect $v_{\Gamma',i}$ and $v_{e,0}$ with $m_e/d_{\Gamma'}$ negative edges and connect $v_{w,\pm}$ and $v_{e,1,\pm}$ with an edge with sign $\pm$.

(iii) Let $a \in \mathcal{A}_{g,2}$ and $w = w_a$. The vertex $v_{a,0}$ is connected to both $v_{w,+}$ and $v_{w,-}$ by a positive edge.

**6.3 Theorem.** *The boundary of the Milnor fiber of the singularity* $f(x,y) + zg(x,y) = 0$ *at the origin is a plumbed manifold with plumbing graph* $G$.

**6.4 Remark.** (i) Let $a \in \mathcal{A}_{g,2}$ and assume that $l_a = 1$. In this case, the vertices $v_{a,1}, \ldots, v_{a,m}$, where $w = w_a$ and $m = m_w$, blow down to simplify the graph (see [13] for blowing down). This operation removes these vertices, and replaces the Euler number $-b_{a,0} = 0$ with $-b_{a,0} = m$.

(ii) We can apply the operation R0(a) from [13] to the vertices $v_{\Gamma',i}$ for a connected component $\Gamma' \subset \Gamma_1$ as well as to $v_{a,i}$ for $a \in \mathcal{A}_{g,2}$ and $1 \leq i \leq m_{w_a}$. This way, all the edges adjacent to these vertices will be positive instead of negative. Note, however, that this also changes the sign of the corresponding multiplicities given in section 7.

## 7 A multiplicity system for $z$

In this section, we give multiplicities and dual multiplicities for the function $z$. For simplicity, the multiplicitiy and dual multiplicity for a vertex $v_*$ constructed in definition 6.1 will be denoted by $m_*$ and $n_*$. The proof of theorem 7.1 is given in section 9.

**7.1 Theorem.** *The restriction* $z|_M$ *of the coordinate function* $z$ *to the boundary* $M = \partial F_\Phi$ *of the Milnor fiber of* $\Phi$ *satisfies the conditions given in 4.1. Furthermore, the associated families of multiplicities* $(m_v)_{v \in \mathcal{V}(G)}$ *and dual multiplicities* $(n_v)_{v \in \mathcal{W}(G)}$ *are is given as follows.*

*(i) If* $\Gamma' \subset \Gamma_1$ *is a connected component, then* $m_v = 1$ *and* $n_v = 0$ *for* $v = v_{\Gamma',i}$, $i = 1, \ldots, d_{\Gamma'}$.

*(ii) Let* $a \in \mathcal{A}_{1,f}$ *be an arrowhead connected to* $w \in \mathcal{W}_1$ *in* $\Gamma$ *and set* $\tilde{m}_w = m_w / \gcd(m_w, m_a)$ *and* $\tilde{m}_a = m_a / \gcd(m_w, m_a)$. *Write* $m_w/m_a = \tilde{m}_w/\tilde{m}_a = [k_1, \ldots, k_s]$ *and define* $\mu_i, \tilde{\mu}_i$ *as in 5.1. The multiplicities of* $z$ *are given by*

$$m_{a,i,+} = (m_w - l_w)\mu_i - m_a\tilde{\mu}_i, \quad m_{a,i,-} = l_w\mu_i$$

*for* $i = 1, \ldots, s$ *and* $m_{a,0} = -\tilde{m}_a l_w$. *The dual multiplicities for these vertices are given by* $n_{a,1,+} = m_a$, *and* $0$ *otherwise.*

*(iii) Let* $v_1, v_2$ *and* $e$ *be as in definition 6.1(iii). Let* $\tilde{m}_i = m_{v_i} / \gcd(m_{v_1}, m_{v_2})$ *for* $i = 1, 2$. *Write* $m_{v_2}/m_{v_1} = \tilde{m}_2/\tilde{m}_1 = [k_1, \ldots, k_s]$ *and define* $\mu_i, \tilde{\mu}_i$ *for* $i = 1, \ldots, s$ *as in 5.1. Then* $m_{e,0} = \tilde{m}_1 l_{v_2} - \tilde{m}_2 l_{v_1}$ *and*

$$m_{e,i,+} = (m_{v_1} - l_{v_1})\mu_i - (m_{v_2} - l_{v_2})\tilde{\mu}_i, \quad m_{e,i,-} = l_{v_1}\mu_i - l_{v_2}\tilde{\mu}_i$$

*The dual multiplicities vanish on these vertices.*

*(iv) Let* $w \in \mathcal{W}_2$. *Then* $m_{w,+} = m_w - l_w$ *and* $m_{w,-} = l_w$. *The dual multiplicities are given by* $n_{w,+} = \sum_{w_a = w} m_a$ *and* $n_{w,-} = 0$.

*(v) Let* $a \in \mathcal{A}_{g,2}$ *and set* $w = w_a$. *Then* $m_{a,0} = -l_a$ *and* $m_{a,i} = 1$ *for* $i = 1, \ldots, m_w$. *The dual multiplicities associated with* $v_{a,i}$ *vanish.*

**7.2 Remark.** Let $e, v_1$ be as in theorem 7.1(iii). One proves that, in fact, $m_{e,1,+} = m_{v_1} - l_{v_1}$ and $m_{e,1,-} = l_{v_1}$.

## 8 Examples

**8.1 Example.** The singularity $T_{a,b,\infty}$ is the singularity at the origin of the hypersurface given by $x^a + y^b + xyz = 0$. In the case $b = 2$, the boundary of the Milnor fiber has been described in [12]. We take $f(x, y) = x^a + y^b$ and $g(x, y) = xy$. We will assume $a, b$ satisfying $a \geq b \geq 2$ and $a > 2$. We claim that the boundary of the Milnor fiber of this singularity is given by the plumbing graph

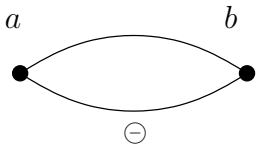


$$f(x, y) = x^a + y^b$$
$$g(x, y) = xy$$

Figure 8: A plumbing graph for the boundary of the Milnor fiber of the singularity $T_{a,b,\infty}$, $x^a + y^b + xyz$.

If $b > 2$, then the minimal graph representing this plumbed manifold is a cycle having two vertices with Euler number $-3$, connected by two bamboos of $(-2)$-vertices of length $a - 3$ and $b - 3$. If $b = 2$, then the minimal graph has one vertex with Euler number $-4$, and a bamboo starting and ending at this vertex, consisting of $a - 3$ verties with Euler number $-2$. In either case, all genera vanish, and the cycle has one edge (or any odd number of edges) with decoration $-1$.

Let $\phi : V \to \mathbb{C}^2$ be the minimal resolution of the plane curve $fg$ and let $\Gamma$ be its resolution graph. Then $\Gamma$ is a string with two arrowheads corresponding to $g$, one on each end of the string, as well as $d := \gcd(a, b)$ arrowheads corresponding to $f$. Name the nonarrowhead vertices of the graph $v_1, \ldots, v_s$ so that $v_i, v_{i+1}$ are adjacent. Let $-b_i$ be the selfintersection number associated with the vertex $v_i$. There is a unique $j$ so that $-b_j = -1$. The set $\mathcal{A}_f$ consists of $d$ arrowheads, each connected to $v_j$, whereas $\mathcal{A}_g$ consists of two arrowheads, one connected to $v_1$ and the other to $v_s$. Write also $m_i, l_i$ for the multiplicities of $f$ and $g$ on $v_i$.

*Claim:* We have $m_1 \geq l_1$ and $m_s \geq l_s$ and $m_i > l_i$ for $i = 2, \ldots, s - 1$.

In fact, using [4, Lemma 20.2], one finds $m_j = ab/d$ and $l_j = a/d + b/d$. It follows from our assumptions that $m_j - l_j > 0$. Now, define integers $r_i = m_i - l_i$ for $i = 1, \ldots, s$ and $r_0 = r_{s+1} = -1$. We then have

$$r_{i-1} - b_i r_i + r_{i+1} = 0, \quad i = 1, \ldots, \hat{j}, \ldots, s.$$

It follows easily that this sequence increases strictly from $r_0 = -1$ to $r_j = m_j - l_j$, and then decreases strictly from $r_j$ to $r_{s+1} = -1$. Since these are integers, the claim follows.

We leave to the reader to show that the equality $m_i = l_i$ holds for $i = 1$ or $i = s$ if and only if $b = 2$, the case already covered by Némethi and Szilárd [12]. This can be achieved by calculating $m_i$ and $l_i$ explicitly using Lemma 20.2 of [4].

We start by showing how the above graph is obtained from the output of the algorithm in the case when $l_i > m_i$ for all $i$. Since $\mathcal{W} = \mathcal{W}_2$, the graph $G_2$ consists of two strings, one of them identical to $\Gamma$, the other one having

Euler numbers with opposite signs and negative edges. In addition, we have $\mathcal{A}_{g,2} = \{a_x, a_y\}$, two arrowhead vertices corresponding to the strict transform of the factors $x$ and $y$ of $g$. As described in remark 6.4, the graph $\Gamma$ can be taken as these two strings, connected on each end by vertices with Euler number $m_x$ and $m_y$. These are the multiplicities of $f$ along the components on the end of the string. It follows from [4] that these multiplicities are $a$ and $b$. Furthermore, the two strings blow down (we can blow down the vertices one by one in the opposite order in which they appear during the process of resolving $f$). Each string is replaced by an edge, the first string by a positive edge, the second one by a negative edge. Below, we explicate the case when $a = 7$ and $b = 5$.

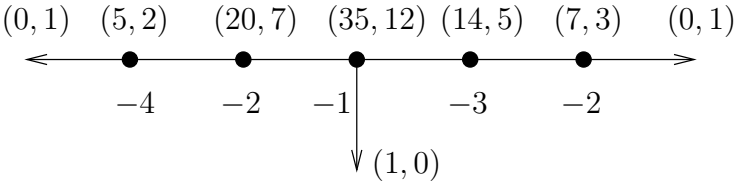


Figure 9: A resolution graph of the plane curves $f(x, y) = x^7 + y^5 = 0$ and $g(x, y) = xy$, along with their multiplicities.

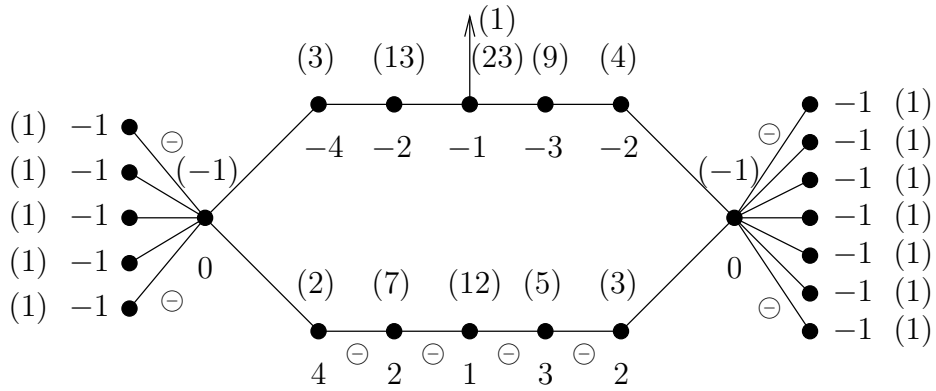


Figure 10: Output of the algorithm for $\Phi(x, y, z) = x^7 + y^5 + xyz$.

In the case when either $m_1 = l_1$ or $m_s = l_s$, the algorithm has, in fact, the same output. We let it suffice to clarify this principle by considering an example. Take $a = 3$ and $b = 2$. A resolution graph $\Gamma$, decorated with the pairs of multiplicities $(m_v, l_v)$ is shown in fig. 11.

We see that $\mathcal{W}_2$ now only contains the vertex $v_2$, whereas $v_1, v_3 \in \mathcal{W}_1$, each providing a connected component of $\Gamma_1$. We order the vertices in fig. 11 in such a way that $b_1 = -2$ and $b_3 = -3$. Applying definition 6.1(i) to the component $\Gamma'$ of $\Gamma_1$, containing only the vertex $v_1$, as well as $\Gamma''$ containing only $v_3$, we get

$$d_{\Gamma'} = 3, \quad g_{\Gamma'} = 0, \quad -b_{\Gamma'} = -1, \quad d_{\Gamma''} = 2, \quad g_{\Gamma''} = 0, \quad -b_{\Gamma''} = -1.$$

We get five new vertices. The edges $e_1 = \{v_1, v_2\}$ and $e_2 = \{v_2, v_3\}$ are of the

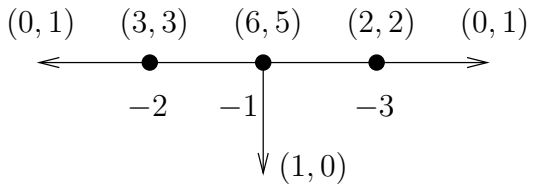


Figure 11: A resolution graph of the plane curves $f(x, y) = x^3 + y^2 = 0$ and $g(x, y) = xy$, along with their multiplicities.

form described in definition 6.1(iii). The five new vertices are connected to $v_{e_1,0}$ and $v_{e_2,0}$ to obtain the graph in fig. 12, which also shows the multiplicities of the function $z$. After blowing down, we obtain fig. 8.

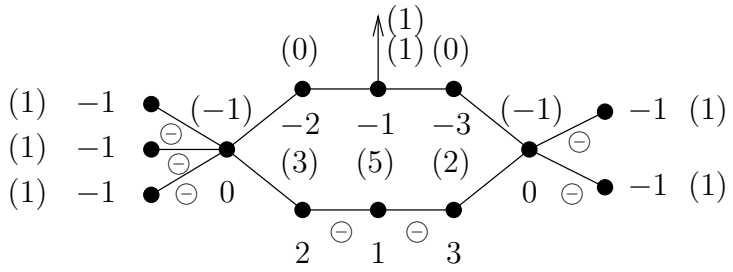


Figure 12: Output of the algorithm for $\Phi(x, y, z) = x^3 + y^2 + xyz$.

**8.2 Example.** Consider the plane curves

$$f(x,y) = \left(x^3 + \lambda_1 y^2\right)\left((x^3 + \varpi_1 y^2)^3 + \mu_1 x^{10}\right)^2\left((x^3 + \varpi_2 y^2)^3 + \nu_1 x^{10}\right)^2,$$
$$g(x,y) = \left(x^3 + \lambda_2 y^2\right)^5\left((x^3 + \varpi_1 y^2)^3 + \mu_2 x^{10}\right)\left((x^3 + \varpi_2 y^2)^3 + \nu_2 x^{10}\right),$$

where $\lambda_i, \mu_i, \nu_i, \varpi_i \in \mathbb{C}^*$ are generic. A resolution graph is given in fig. 13.

The output of our algorithm is shown in fig. 14. The connected graph $\Gamma' = \Gamma_1$ consists of the three nonarrowheads to the left, yielding numerical data

$$d_{\Gamma'} = 1, \quad g_{\Gamma'} = 57, \quad -b_{\Gamma'} = -270.$$

Correspondingly, fig. 14 has one vertex decorated with genus 57 and Euler number $-270$.

The set $\mathcal{A}_{f,1}$ contains one element. The relevant data for this edge is $m_a = 1$ and $m_w = 54$. The negative continued fraction expansion of $1/54$ consists of a $-1$, followed by 53 copies of $-2$. As a result, we obtain the graph $G_{f,1}$ seen to the left in fig. 14.

To the right of $v_{\Gamma',1}$ in fig. 14, we see the two identical components of $G_{\mathrm{b}}$, each consisting of a 0-vertex, and two strings obtained from the fraction $m_{v_2}/m_{v_1} = 58/54 = 29/27$, whose negative continued fraction expansion consists of 13 copies of $-2$, followed by a $-3$ (note that in fig. 14, this $\pm 3$ is to the left of the $\pm 2$'s, the $\pm 3$ to the right belongs to $G_2$).

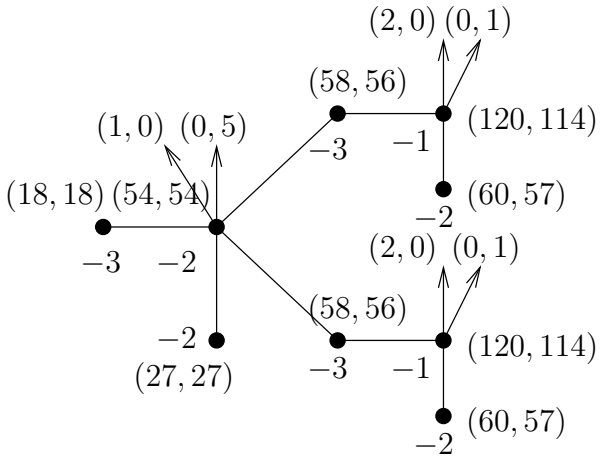


Figure 13: Plane curves whose branches have 1 and 2 Puiseux pairs.

To the right of $G_{\mathrm{b}}$ in fig. 14 we see the graph $G_2$ obtained from the two identical components of $\Gamma_2$, each consisting of three vertices with Euler numbers $-3, -1, -2$.

Finally, to the right in fig. 14 we find the two identical components of $G_{g,2}$. Each component has a 0-vertex, and 120 copies of $(-1)$-vertices.

This graph is not in normal form in the sense of [13]. Let us apply Neumann's algorithm. Start by blowing down the $-1$- and 1-vertices on the left. This yields new $-1$ and 1-vertices. Blowing down in total 106 times, all that is left of $G_{f,1}$ is a 0-vertex. We can thus apply *splitting*, or Neumann's operation R6. In his notation (p. 305-306) we have $s = 2$ and $k_1 = k_2 = 2$ and

$$k = 2g_{\Gamma'} + \sum_{j=1}^{s}(k_j - 1) = 116.$$

As a result, the splitting induces 116 singletons with Euler number 0, and the two identical components formed by the graphs $G_{\mathrm{b}}$ and $G_{g,2}$, as well as the four dashed edges to the right.

As the next step, apply 0-*chain absorption*, or operation R3, 16 times to each component. Note that each absorption, the new vertex has Euler number $-b - (-b) = 0$, allowing us to absorb again.

This, in fact, concludes Step 1 of [13], and what is left is the graph we see in fig. 15.

Next, apply Step 2 of [13]. This means replace the 2-vertex with a $-2$-vertex, the 120-vertex with a string, consisting of 119 copies of $-2$-curves, and the 0-vertex with a $-3$-vertex.

Steps 3-6 of Neumann's algorithm do nothing to this output, and therefore we have found the normal form of the output of our algorithm, seen in fig. 16.

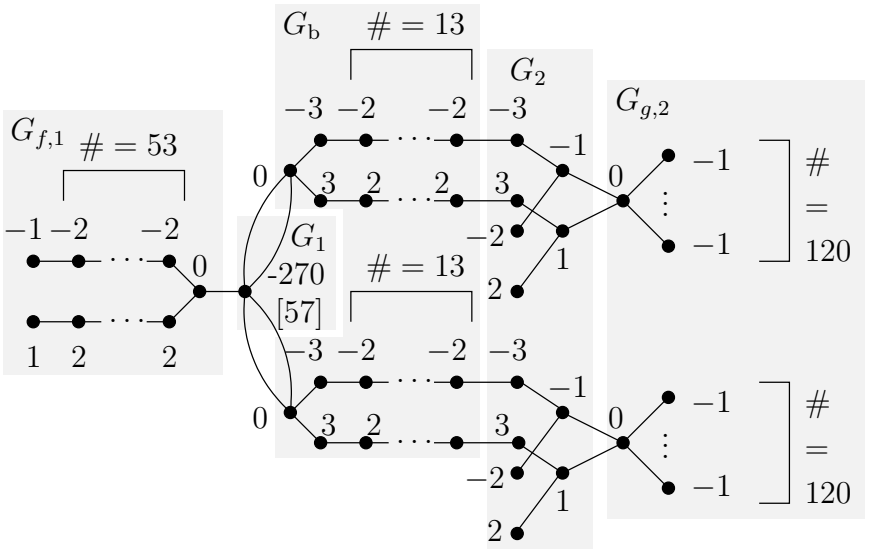


Figure 14: From left to right we see the graphs $G_{f,1}$, $G_1$, $G_{\mathrm{b}}$, $G_2$ and $G_{g,2}$, except that negative signes of edges are not marked. The reader may verify that no negative edge decorations survive to the normal representative below.

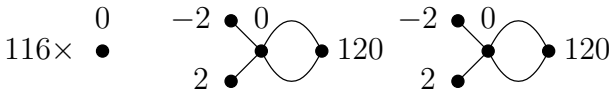


Figure 15: The output of our algorithm, after applying Neumann's Step 1 [13] of determining the normal form.

## 9 Proofs

To prove theorems 6.3 and 7.1, we start by defining pieces $M_v \subset M$ and projections $\pi_v : M_v \to \Sigma_v$ for all vertices $v \in \mathcal{V}$, using the description in theorem 2.5. From the construction, it will be clear that $M = \cup_{v\in\mathcal{V}} M_v$, and that individual pieces intersect according to the edges of $G$. Finally, we verify the formulas for genera and selfintersection numbers. In fact, it will be clear that the genus decoration is zero, except for in the case of $v_{\Gamma'}$, where an argument similar to A'Campo's formula [1] is used. Similarly as in [11, 12], nontrivial Euler numbers are determined using the multiplicities of $z$ and lemma 4.3. We note that the proof of theorem 7.1, can be carried out as soon as the projections $\pi_v$ are defined. In particular, this proof does not use the Euler numbers, which are computed using the multiplicities of $z$.

*Proof of theorem 6.3.* We start by providing sets $M_v$ for each vertex of the graph $G$. We then prove that these pieces provide a plumbing structure on $M$ with the plumbing graph $G$.

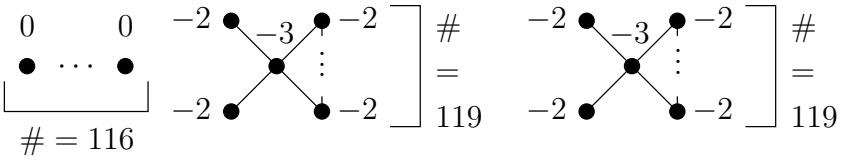


Figure 16: The normal plumbing graph for the boundary of the Milnor fiber of the singularity $f(x,y)+zg(x,y)=0$.

(i) Let $X_1'$ be the closure of the set

$$\overline{T}_{f,g} \cap T_1 \setminus (T_{f,1} \cup T_2).$$

By construction, this is a closed tubular neighbourhood of

$$F_{f,1} := F_f \cap T_1 \setminus (T_{f,1} \cup T_2),$$

in particular, we have a disk bundle $X_1' \to F_{f,1}$. We can assume that the intersection of this disk bundle with the divisor associated with $g$ is a set of disks. Let $X_1$ be the four manifold obtained from $X_1'$ by twisting along these disks as in definition 2.4 and let $M_1 \subset \partial X_1$ be the associated $S^1$ bundle. It is then clear that we have $M_1 \subset M_{f,g}$, that the boundary of $M_1$ consists of tori and that $M_1$ is in a natural way an $S^1$ bundle over $F_{f,1}$.

Let $\Gamma' \subset \Gamma_1$ be a component as in definition 6.1(i). Setting

$$X'_{\Gamma'} = X_1' \cap \bigcup_{v \in \mathcal{V}(\Gamma')} T_v,$$

we obtain correspondingly $X_{\Gamma'} \subset X_1$ and $M_{\Gamma'} \subset M_1$. This way, $M_{\Gamma'}$ is an $S^1$ bundle over the surface $F_{f,\Gamma'} = F_f \cap X'_{\Gamma'}$.

Firstly, we note that the number of connected components of $F_{f,\Gamma'}$ is precisely $d_{\Gamma'}$ and that, furthermore, the monodromy permutes these components cyclically. This follows from Proposition 2.20 of [11], see also 2.21 of the same article.

Secondly, the genus of the components of $F_{f,\Gamma'}$ is $g_{\Gamma'}$, satisfying eq. 6.1. This follows from a small generalization of A'Campo's formula [1] which gives

$$\chi(F_{f,\Gamma'}) = \sum_{v \in \mathcal{V}(\Gamma')} m_v(2 - \hat{\delta}_v).$$

What is more, $F_{f,\Gamma'}$ has $m_e$ boundary components close to the intersection of $E_v$ and $E_{w_e}$ for $e \in \hat{\mathcal{E}}(\Gamma')$. Thus, $F_{f,\Gamma'}$ has a total of $\sum_{e \in \hat{\mathcal{E}}(\Gamma')} m_e$ boundary components.

The formula eq. 6.2 is verified below.

(ii) Let $a \in A_{1,f}$ and set $w = w_a$. Define $M_a = \partial \overline{T}_{f,g} \cap \overline{T}_a$ We have coordinates $u, v$ on $T_a$ so that $T_a \cong \{(u,v) \,|\, |u| \le 1,\ |v| \le 1\}$ and so that $E_a \cap T_a$ and $E_w \cap T_a$ are the vanishing sets of $u$ and $v$, respectively. We can then write $M_a = M_{a,+} \cup M_{a,-} \cup M_{a,0}$ where for certain $0 < \eta \ll \varepsilon \ll 1$, we have

$$M_{a,+} = \{(u,v) \,|\, |v| = 1,\ |u| \le 1\}, \quad M_{a,-} = \{(u,v) \,|\, |v| = \eta,\ |u| \le 1\}$$

and $M_{a,0}$ is defined by setting

$$M'_{a,0} = \{(u,v) \,|\, |u| = 1,\, \eta \leq |v| \leq 1\}\,, \quad M_{a,0} = M'_{a,0} \setminus N,$$

where $N$ is an $\varepsilon$ neighbourhood around $F_f \cap M'_{a,0}$. The projection of this picture via $(u,v) \mapsto (|u|,|v|)$ is shown in fig. 17. We can assume that in the

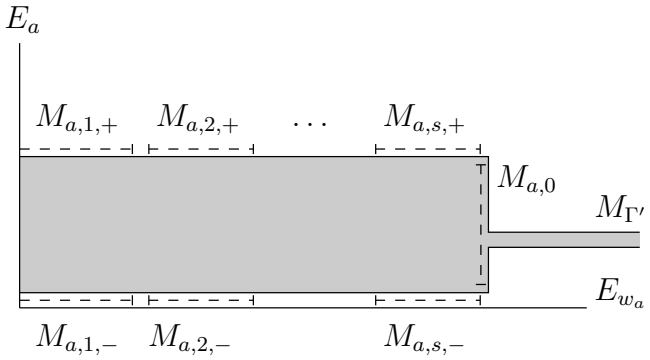


Figure 17: A diagram showing what happens near $E_a \cap E_{w_a}$.

coordinates $u, v$, we can write $f|_{T_a}(u,v) = u^{m_a} v^{m_w}$. Define $\tilde{m}_a = m_a/m_e$ and $\tilde{m}_w = m_w/m_e$. We find

$$F_f \cap M'_{a,0} = \coprod_{j=0}^{m_e-1} \left\{ (e^{(-t+j/m_w)\tilde{m}_w 2\pi i}, e^{t\tilde{m}_a 2\pi i}) \,\middle|\, t \in [0,1] \right\}$$

In fact, we have an $S^1$ bundle projection $\pi'_{a,0}$ mapping $M'_{a,0}$ to an annulus by the formula $\pi'_{a,0}(u,v) = u^{\tilde{m}_a} v^{\tilde{m}_v}$. This way, $F_f \cap M'_{a,0}$ consists of $m_e$ fibers of $\pi'_{0,a}$. In particular, we can assume that $\pi'_{a,0}$ restricts to an $S^1$ bundle $\pi_{0,a} = \pi'_{0,a}|_{M_{0,a}}$. We orient the fibers so that one of them is parametrized as $t \mapsto (t^{-\tilde{m}_w}, t^{\tilde{m}_a})$, which induces an orientation on the target space of $\pi_{0,a}$.

By lemma 5.4, the manifold $M_{a,+}$ can be given as a plumbed manifold with plumbing graph as in fig. 2, where $[k_1, \ldots, k_s] = m_a/m_w$, so that the section corresponding to the arrowhead to the right can be chosen to coincide with a fiber of $M_{a,0}$, with the opposite orientation. Furthermore, we have an orientation reversing diffeomorphism $M_{a,+} \to M_{a,-}$ given by $(u,v) \mapsto (u, \eta v)$. This way, we see $M_{a,-}$ as a plumbed manifold with the same plumbing graph, modified by changing signs on all selfintersection numbers as well as edges.

At this point, we have shown that the manifold $M_a$ is a plumbed manifold with plumbing graph $G_a$, with $m_e$ dashed arrows added to $v_{a,0}$, except we did not specify a section corresponding to these arrowheads. Furthermore, (and this cannot be done without the sections) we have not determined the Euler number associated with $v_{a,0}$. Since $M_{0,a}$ is obtained by removing a tubular neighbourhood around a fiber of the projection $\pi'_{0,a}$, we can choose as a section a meridian around this fiber. Note that this section is exactly a fiber of the projection $\pi_{\Gamma',i}$ for a suitable $1 \leq i \leq d_{\Gamma'}$, where $w$ is a vertex of the component $\Gamma'$ of $\Gamma_1$. But we can be more specific. Let $\psi : S^1 \to M_{a,+}$ be a parametrization

of a fiber in the boundary component of $M_{a,s,+}$. This induces a map $S_1 \times [\eta, 1] \to M'_{a,0}$ which is a global section to the fibration of $M'_{a,0}$, restricting to a global section to the fibration of $M_{a,0}$, which again restricts to a parametrization of the fibers of $M_{a,s,\pm}$, as well as a parametrization of a meridian around $F_f \cap M_{a,0}$. This shows that with this choice of sections on the boundary, the Euler number of the bundle $M_{a,0}$ is 0.

Finally, we note that $M_{a,0}$ intersects $M_{\Gamma'}$ in exactly $m_e$ tori, and that the number of these tori in each component of $M_{\Gamma'}$ is the same. It follows from the construction that in each of these tori, a fiber of $M_{a,0}$ and a fiber from $M_{\Gamma'}$ form an integral basis on homology. Furthermore, one verifies that an oriented fiber of $M_{a,0}$ in such a torus is an oriented section of $M_{\Gamma'}$. This can be seen by noting that both wind around $E_a$ with multiplicity $-\tilde{m}_a$. Therefore, these tori yield edges with a negative sign, by lemma 3.8. These are the edges defined in definition 6.2(i).

(iii) Let $e$ and $v_i \in \mathcal{W}_i$ be as in 6.1(iii). Let $D$ be a disc in $E_{v_1}$ with center the intersection point of $E_{v_1}$ and $E_{v_2}$ corresponding to $e$ which is a slightly bigger than the corresponding disk in $E_{v_1} \cap \overline{T}_{v_2}$. We can add the preimage of $D$ in $\overline{T}_{v_1} \setminus T'_{v_2}$ to $\overline{T}_{f,g}$ without changing its diffeomorphism type. From here, the proof follows similarly as in the previous case. A schematic picture is shown in fig. 18.

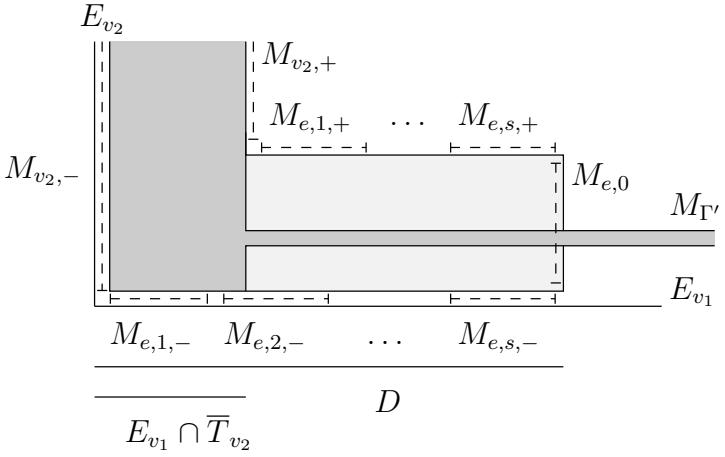


Figure 18: A diagram showing what happens near $E_{v_1} \cap E_{v_2}$.

(iv) Let $w \in \mathcal{W}_2$ and define $M_{w,+}$ as $\partial \overline{T}_w \setminus \cup_v T_v$, where the union $\cup_v$ ranges over $v \in \mathcal{W} \cup \mathcal{A}_g \setminus \{w\}$. Similarly, define $M_{w,-}$ as $\partial \overline{T}'_w \setminus \cup_v T'_v$, for the same index set for $v$, where we take $T'_v = T_v$ if $v \in \mathcal{A}$. Set $M_w = M_{w,+} \cup M_{w,-}$. It follows from construction that $M_w$ consists of two $S^1$ bundles over the surface $E_w$ with a disk removed for each neighbour in $\mathcal{W} \cup \mathcal{A}_g \setminus \{w\}$. Indeed, these are the corresponding subsets of the boundaries of $T_w$ and $T'_w$ (recall definition 2.2). These fibrations correspond to the vertices $v_{w,\pm}$.

These fibrations extends canonically over the disks removed from $E_w$ by taking $T_w$ and $T'_w$, and we can take a meridians around central fibers as the trivializing

section on the boundary. It follows immediately that the two $S^1$ bundles have relative Euler numbers $-b_{w,\pm} = \mp b_w$. Furthermore, since $E_w$ is a rational curve, the two vertices $v_{w,\pm}$ have associated genus 0.

As both components of $M_w$ are boundaries of similar tubular neighbourhoods, they can be identified, but the inner one, i.e. the boundary of $T'_w$ has its orientation reversed. We will consider this part as a fibration over the same base as the outer component. Therefore, a fiber in $M_{w,+}$ is a meridian around $E_w$, whereas a fiber in $M_{w,-}$ is a (relatively small) meridian around $E_w$ with the orientation reversed.

If $w, w' \in \mathcal{W}_2$ are joined by an edge, it follows easily that the two components corresponding to $w$ intersect with those of $w'$ in the way as prescribed by the resolution graph $\Gamma$.

(v) Finally, we describe what happens close to a component of the strict transform of $g$ corresponding to $a \in \mathcal{A}_{g,2}$.

Let $M'_a = M' \cap \overline{T}_a$ and $M_a$ the corresponding twisted subset of $M$. Let $M_{a,0} = M \cap \partial T_a$. It follows from construction that $M_a$ fibers by a map $\pi_{a,0}$ over the disk $E_a$ with $m_a + 1$ smaller disks removed, one corresponding to $T'_{w_a}$, and $m_a$ of them corresponding to $T_\varepsilon$. We orient the fiber to coincide with that of a meridian around $E_a$. This chooses an orientation of the base space of $\pi_{a,0}$, the opposite of the standard one on $E_a$. This bundle is trivialized in a similar way as in (ii), yielding Euler number $-b_{a,0} = 0$. It is also clear that $g_{a,0} = 0$.

The closure of $M_a \setminus M_{a,0}$ is an $S^1$ bundle over $F_f \cap T_a \cong \amalg_{m_w} \overline{D}$. This gives $m_w$ pieces $M_{a,1}, \ldots, M_{a,m_w}$, ordered arbitrarily. The fibers are meridians around $F_f$.

We see that $M_a$ is a plumbed manifold with plumbing graph $G_a$ (with some dashed arrows added, corresponding to the boundary). Using lemma 3.8, we see that the edges between $v_{a,0}$ and $v_{a,i}$ have a negative sign, whereas the edges connecting $v_{a,0}$ and $v_{w,\pm}$ are positive.

In (i-v) above we have assigned subsets $M_v \subset M$ to each vertex $v$ of the graph $G$ constructed in definitions 6.1 and 6.2. It is clear that each piece is connected and that each boundary components of any of the pieces are tori. Furthermore, the components of intersection of two pieces correspond to the edges connecting the corresponding vertices. The base space of each fibration is a surface of the genus specified, or zero otherwise.

The only part which remains to prove is eq. 6.2. But this follows immediately from lemma 4.3 and theorem 7.1. ■

*Proof of theorem 7.1.* (i) Let $\Gamma'$ be as in definition 6.1(i). It follows from the proof of Theorem 4.1(ii) in [14] that $|z|$ is constant on $M_{\Gamma',i}$ (and nonzero). It follows that the dual multiplicities $n_{\Gamma',i}$ vanish. A fiber in $M_{\Gamma',i}$ is an oriented meridian around $F_f$. The restriction of $z = (f - \varepsilon)/g$ to such a fiber is a map of degree 1, thus $m_{\Gamma',i} = 1$.

(ii) Let $a \in \mathcal{A}_{1,f}$ as in definition 6.1(ii). We start by observing that the vanishing set of the function $z = (f - \varepsilon)/g$ is contained in the piece $M_{a,1,+}$. The vanishing set of $z$ is the Milnor fiber $F_f$ of $f$. The intersection $F_f \cap \partial T_a$ consists of two parts, contained in neighbourhoods around $E_w \cap \partial T_a$ and $E_a \cap \partial T_w$. By construction, the former is not included in $M_a$. The latter is homologous to

a meridian around $E_w$ with multiplicity $m_w$. We can take this meridian as $E_a \cap \partial T_a$. Therefore, the dual multiplicities vanish on all vertices of $G_a$ except for $v_{a,1,+}$ and we have $n_{a,1,+} = m_a$.

It follows from the explicit calculations in (ii) in the proof of theorem 6.3 that the restriction of $f - \varepsilon$ to a fiber of $M_{a,0}$ has degree zero. Indeed, in the coordinates $u, v$ introduced there for the polydisk $T_a$, we have $f|_{T_a} = u^{m_a} v^{m_w}$ and a fiber in $M_{a,0}$ is parametrized in these coordinates by $[0,1] \to T_a$, $t \mapsto (e^{-t\tilde{m}_w 2\pi i}, e^{t\tilde{m}_a 2\pi i})$. Since $g$ vanishes with order $l_w$ along $E_w$, and does not vanish along $E_a$, it follows that the multiplicity $m_{a,0}$ equals $-l_w\tilde{m}_a$.

Now, the sequence $m_{a,i,+}$, $i = 1, \ldots, s$ satisfies

$$\begin{array}{rcrcrcll} & - & b_{a,1,+}m_{a,1,+} & + & m_{a,2,+} & = & n_{a,+,1}, & \\ m_{a,i-1,+} & - & b_{a,i,+}m_{a,i,+} & + & m_{a,i+1,+} & = & 0, & i = 2, \ldots, s-1, \\ m_{a,s-1,+} & - & b_{a,s,+}m_{a,s,+} & & & = & m_{a,0}. & \end{array} \tag{9.1}$$

The same equations are satisfied by the sequence $(l_w - \tilde{m}_w)\mu_i - m_a\tilde{\mu}_i$, as is easily checked. It follows that the two sequences coincide, since the matrix associated with this system of linear equations is negative definite. A similar argument proves the statement for the multiplicities $m_{a,i,-}$.

(iii) Let $e$ be an edge in $G$ connecting $v_1$ and $v_2$ as in definition 6.1(iii). We start by observing that $z$ does not vanish on $M_e$, and so all dual multiplicities vanish for the vertices of $G_e$.

Similarly as above, we find that the map $f - \varepsilon$ restricted to a fiber $C_{e,0} \subset M_{e,0}$ has degree zero, and $g$ has degree $\tilde{m}_2 l_{v_1} - \tilde{m}_1 l_{v_2}$. It follows that $m_{e,0} = \tilde{m}_1 l_{v_2} - \tilde{m}_2 l_{v_1}$. Now, similar reasoning as above determines the multiplicities $m_{e,i,\pm}$. Namely, we have linear equations

$$\begin{array}{rcrcrcll} & - & b_{e,1,\pm}m_{e,1,\pm} & + & m_{e,2,\pm} & = & m_{e,0}, & \\ m_{e,i-1,\pm} & - & b_{e,i,\pm}m_{e,i,\pm} & + & m_{e,i+1,\pm} & = & 0, & i = 2, \ldots, s-1, \\ m_{e,s-1,\pm} & - & b_{e,s,\pm}m_{e,s,\pm} & & & = & m_{w_2,\pm}. & \end{array} \tag{9.2}$$

The result follows as soon as we determine the multiplicities $m_{w_2,\pm}$:

(iv) Let $w \in \mathcal{W}_2$. Above, we have determined that $C_{w,-}$ is a meridian around $E_w$, small with respect to $\varepsilon$ and having the opposite orientation than the standard meridian. It follows that $z = (f - \varepsilon)/g$ restricted to $C_{w,-}$ has degree $l_w$, i.e. $m_{w,-} = l_w$. Furthermore, $z$ does not vanish on $M_{w,-}$, thus $n_{w,0} = 0$.

On the other hand, $C_{w,+}$ is an oriented meridian around $E_w$, with respect to which $\varepsilon$ is chosen small. It follws that $m_{w,+} = m_w - l_w$. Furthermore, the vanishing set of $z$ in $M_{w,+}$ is homologous to the strict transform of $f$, with multiplicities. Therefore, each $a \in \mathcal{A}_{f,2}$ contributes $m_a$ to $n_{w,+}$, resulting in the sum given.

(v) Let $a \in \mathcal{A}_{g,2}$ and set $w = w_a$. Similarly as in (i), we find that $z$ does not vanish on $M_a$. Therefore, $n_{a,i} = 0$ for $i = 0, \ldots, m_w$. In (v) of the proof of theorem 6.3 we found that $C_{a,0}$ is a meridian around $E_a$. We can assume that the restriction of $f - \varepsilon$ to such a meridian has degree 0. It is also clear that $g$ restricts to a degree $-l_a$ map on such a fiber. It follows that $m_{a,0} = -l_a$.

For $i = 1, \ldots, m_w$, the fiber $C_{a,i}$ is a small meridian around $F_f$. It follows that $m_{a,i} = 1$. ∎

## References


[1] Norbert A'Campo. La fonction zêta d'une monodromie. *Comment. Math. Helv.*, 50:233–248, 1975.

[2] Wolf P. Barth, Klaus Hulek, Chris A. M. Peters, and Antonius Van de Ven. *Compact complex surfaces*. Berlin: Springer, 2nd enlarged ed. edition, 2004.

[3] T. de Jong and D. van Straten. Deformation theory of sandwiched singularities. *Duke Math. J.*, 95(3):451–522, 1998.

[4] David Eisenbud and Walter D. Neumann. *Three-dimensional link theory and invariants of plane curve singularities.*, volume 110 of *Annals of Mathematics Studies*. Princeton University Press, 1985.

[5] Javier Fernández de Bobadilla and Aurélio Menegon Neto. The boundary of the Milnor fibre of complex and real analytic non-isolated singularities. *Geom. Dedicata*, 173:143–162, 2014.

[6] Françoise Michel and Anne Pichon. On the boundary of the Milnor fibre of nonisolated singularities. *Int. Math. Res. Not.*, 2003(43):2305–2311, 2003.

[7] Françoise Michel and Anne Pichon. Carrousel in family and non-isolated hypersurface singularities in $\mathbb{C}^3$. *J. Reine Angew. Math.*, 720:1–32, 2016.

[8] Françoise Michel, Anne Pichon, and Claude Weber. The boundary of the Milnor fiber of Hirzebruch surface singularities. In *Singularity theory. Proceedings of the 2005 Marseille singularity school and conference*, pages 745–760. Singapore: World Scientific, 2007.

[9] Françoise Michel, Anne Pichon, and Claude Weber. The boundary of the Milnor fiber for some non-isolated singularities of complex surfaces. *Osaka J. Math.*, 46(1):291–316, 2009.

[10] David B. Mumford. The topology of normal singularities of an algebraic surface and a criterion for simplicity. *Publ. Math., Inst. Hautes Étud. Sci.*, 9:5–22, 1961.

[11] András Némethi. Resolution graphs of some surface singularities. I: Cyclic coverings. In *Singularities in algebraic and analytic geometry. Papers from the AMS special session, San Antonio, TX, USA, January 13-14, 1999*, pages 89–128. Providence, RI: American Mathematical Society (AMS), 2000.

[12] András Némethi and Ágnes Szilárd. *Milnor fiber boundary of a non-isolated surface singularity*, volume 2037 of *Lecture Notes in Math.* Springer, Heidelberg, 2012.

[13] Walter D. Neumann. A calculus for plumbing applied to the topology of complex surface singularities and degenerating complex curves. *Trans. Am. Math. Soc.*, 268:299–343, 1981.

[14] Baldur Sigurðsson. The Milnor fiber of the singularity $f(x,y)+zg(x,y)=0$. *Revista Matemática Complutense*, 29(1):225–239, 2016.